Gauge-invariant three-boson vertices in the standard model and the static properties of the W

Joannis Papavassiliou and Kostas Philippides
Department of Physics, New York University, 4 Washington Place, New York, New York 10003
(Received 5 April 1993)

We use the S-matrix pinch technique to derive to one-loop order gauge-independent γW^+W^- and ZW^+W^- vertices in the context of the standard model, with all three incoming momenta off shell. We show that the γW^+W^- vertex so constructed is related to the gauge-independent W self-energy, derived by Degrassi and Sirlin, by a very simple QED-like Ward identity. The same results are obtained by the pinch technique applied directly to the process $e^+e^-\to W^+W^-$. Explicit calculations give rise to expressions for static properties of the W gauge bosons such as the magnetic dipole and electric quadrupole moments, which satisfy the crucial properties of infrared finiteness as well as gauge independence.

PACS number(s): 11.15.Bt, 11.15.Ex, 13.40.Fn, 14.80.Er

I. INTRODUCTION

The widespread belief of theoreticians that the standard model of electroweak interactions serves as an effective low-energy description of an underlying more fundamental theory has been persistently denied confirmation for several years, mainly because of the model's impressive agreement with a large body of precise experimental results [1]. This fact, combined with the elusiveness of the top quark and Higgs particles, has motivated the design of a new generation of machines, which will further probe the underpinnings of the standard model in the near future. A new and largely unexplored frontier, on which this ongoing search for new physics will soon focus, is the study of the structure of the three-boson couplings. Since these couplings lie in the heart of the non-Abelian nature of the theory, a systematic confrontation of the standard model predictions in this domain with experiment might shed some light on the underlying structure of the theory, if any.

Motivated by scattering experiments of the form $e^+e^-\to W^+W^-$, the standard parametrization for the most general W^+W^-V vertex with the W's on shell and V offshell, where V stands for γ or Z, is [2–7]

$$\Gamma^V_{\mu\alpha\beta}=-ig_V\left[f[2g_{\alpha\beta}\Delta_\mu+4(g_{\alpha\mu}Q_\beta-g_{\beta\mu}Q_\alpha)]+2\Delta\kappa_V(g_{\alpha\mu}Q_\beta-g_{\beta\mu}Q_\alpha)+4\frac{\Delta Q_V}{M_W^2}(\Delta_\mu Q_\alpha Q_\beta-\tfrac{1}{2}Q^2g_{\alpha\beta}\Delta_\mu)\right]+\cdots , \tag{1.1}$$

with $g_\gamma=gs$ and $g_Z=gc$, where g is the SU(2) gauge coupling and $s\equiv\sin\theta_W$ and $c\equiv\cos\theta_W$, and the dots denote omission of C- or P-violating terms. The four-momenta Q and Δ, first introduced in [8], are related to the incoming momenta q,p_1, and p_2 by $q=2Q,p_1=-\Delta-Q$, and $p_2=\Delta-Q$, as shown in Fig. 1. The quantities $\Delta\kappa_V$ and ΔQ_V are defined as

$$\Delta\kappa_V=\kappa_V+\lambda_V-1 \tag{1.2}$$

and

$$\Delta Q_V=-2\lambda_V , \tag{1.3}$$

where κ_V and λ_V are form factors compatible with C, P, and T invariance. In particular, κ_γ and λ_γ are related to the magnetic dipole moment μ_W and the electric quadrupole moment Q_W, by the expressions

$$\mu_W=\frac{e}{2M_W}(1+\kappa_\gamma+\lambda_\gamma) \tag{1.4}$$

and

$$Q_W=-\frac{e}{M_W^2}(\kappa_\gamma-\lambda_\gamma) . \tag{1.5}$$

In the context of the standard model, the tree level values of the parameters defined above are $f=1$, $\Delta\kappa_V=\Delta Q_V=0$, $\kappa_\gamma=1$, and $\lambda_\gamma=0$. Given the expected experimental precision, and assuming that such quantities can actually be extracted from suitable scattering experiments, calculating the one-loop corrections to these

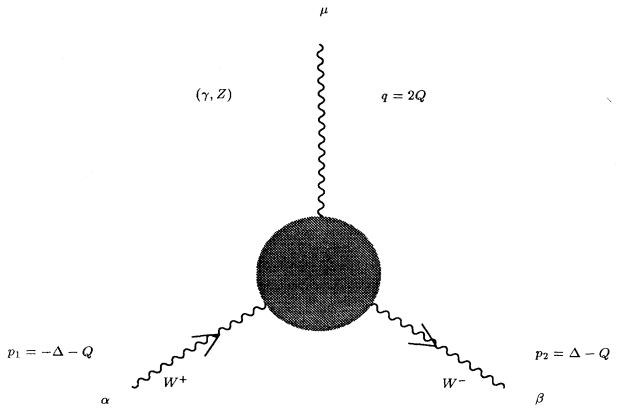

FIG. 1. The kinematics of the VW^+W^- vertex. All momenta are incoming.

parameters is the next necessary step. One then must cast the resulting expressions in the form

$$\Gamma^V_{\mu\alpha\beta} = -ig_V[a_1^V g_{\alpha\beta}\Delta_\mu + a_2^V(g_{\alpha\mu}Q_\beta - g_{\beta\mu}Q_\alpha) + a_3^V \Delta_\mu Q_\alpha \beta_\beta] , \quad (1.6)$$

where a_1^V, a_2^V, and a_3^V are, in general, complicated functions of the momentum transfer Q^2 and the masses of the particles appearing in the loops. It then follows that $\Delta\kappa_V$ and ΔQ_V are given by expressions

$$\Delta\kappa_V = \tfrac{1}{2}(a_2^V - 2a_1^V - Q^2 a_3^V) \quad (1.7)$$

and

$$\Delta Q_V = \frac{M_W^2}{4} a_3^V . \quad (1.8)$$

Calculating the one-loop expressions for $\Delta\kappa_V$ and ΔQ_V is a nontrivial task, not only from the technical point of view, but from the conceptual point of view as well. So, if one proceeded to calculate just the Feynman diagrams contributing to the $\gamma W^+ W^-$ vertex, for example, and then extract from them the contributions to $\Delta\kappa_\gamma$, and ΔQ_γ, after a considerable amount of labor one would arrive at expressions that are plagued with several pathologies, gauge dependence being one of them. Indeed, even if the two W are considered to be on shell, since the incoming photon is not, there is no *a priori* reason why a gauge-independent answer should emerge. In the context of the renormalizable gauges (usually referred to as R_ξ gauges) the final answer depends on the choice of the gauge-fixing parameter ξ, which enters into the one-loop calculations through the gauge-boson propagators (W, Z, γ, and unphysical Higgs particles). In addition, as it was realized by the authors of [7], who, unaware of the fact that there is no gauge cancellation, performed the calculation in the Feynman–t'Hooft gauge ($\xi = 1$), the answer also turns out to be *infrared divergent.* Put in the standard language, the functions $a_i(Q)$ emerging out of this procedure are in general gauge dependent and infrared divergent, and these problems persist *even* when one combines them to form $\Delta\kappa_\gamma$ and ΔQ_γ, according to Eqs. (1.7) and (1.8) (the resulting expressions are, however, ultraviolet finite). Clearly, regardless of the measurability of quantities such as $\Delta\kappa_\gamma$ and ΔQ_γ, from the theoretical point of view one should at least be able to satisfy such crucial requirements as gauge independence and infrared finiteness, when calculating the model's prediction for them.

This unsatisfactory state of affairs, which occurs each time one tries to isolate a particular piece of an S matrix without enough care, can be avoided if one adopts the pinch technique (PT). The PT was invented by Cornwall over a decade ago [9] and has since been applied to a variety of physical problems. The main idea of this method is to resum via a well-defined algorithm the Feynman diagrams contributing to a gauge-invariant process (such as an S-matrix element) in such a way as to form new gauge-invariant vertices, and new propagators with gauge-independent self-energies and only a trivial gauge dependence—that of their tree level parts. In the context of QCD a gauge-invariant gluon self-energy was derived, and its Schwinger-Dyson equation constructed and solved for $T=0$ [10], as well as finite T [11]. The plasmon decay rate was also calculated at finite T using the same method [12]. Later the QCD gauge-invariant three-gluon vertex was calculated at one-loop level and was shown to satisfy a very simple Ward identity [13]. The subleading corrections to the self-energy were calculated by Lavelle [14]. Finally, the gauge-invariant four-gluon QCD vertex was constructed and its Ward identity derived [15]. The PT was first extended to the case of non-Abelian gauge theories with spontaneously broken gauge symmetry (with elementary Higgs bosons) in the context of a toy field theory based on SU(2), and a gauge-independent electromagnetic form factor for the standard model neutrino was constructed [16]. The complicated task of applying the PT in the electroweak sector of the standard model was recently accomplished by Degrassi and Sirlin [17]. These last authors, in addition to deriving explicit expressions for the one-loop gauge-invariant WW and ZZ self-energies, introduced an alternative description of PT in terms of equal time commutators of currents.

In this paper we use the S-matrix PT to construct in the context of the standard model [18], to one-loop order in perturbation theory, a *gauge-invariant* effective γWW vertex with *all three* incoming momenta being *off shell.* The outline of the construction of such a vertex was already given in [17], but no explicit results were reported. It turns out that the vertex $\hat{\Gamma}_{\mu\alpha\beta}(q, p_1, p_2)$ so constructed satisfies a very simple QED-like Ward identity, which relates it to the *gauge-independent* WW self-energy $\hat{\Pi}_{\alpha\beta}$ derived in [17]: namely,

$$q^\mu \hat{\Gamma}_{\mu\alpha\beta} = \hat{\Pi}_{\alpha\beta}(p_1) - \hat{\Pi}_{\alpha\beta}(p_2) , \quad (1.9)$$

where q is the four-momentum of the incoming photon, and p_1 and p_2 of the incoming W^+ and W^-, respectively. Having constructed a gauge-independent vertex for the general case of off-shell momenta we can recover as a special limit the case of interest (W^+ and W^- on shell) by setting $p_1^2 \to M_W^2$ and $p_2^2 \to M_W^2$ and contracting the result with the polarization vectors $\epsilon^\alpha(p_1)$ and $\epsilon^\beta(p_2)$. Finally, projecting out the kinematically relevant pieces according to Eq. (1.6) gives rise to new individually *gauge-independent* and *infrared finite* functions $\hat{a}_i(Q^2)$. So, the additional (ultraviolet finite) pinch contributions not only contain the right terms to cancel all gauge dependences, but they also contribute infrared divergent terms, which *exactly* cancel against the infrared divergences contained in the standard vertex graphs. Combining now the new functions $\hat{a}_i(Q^2)$ according to Eqs. (1.7) and (1.8) we find expressions for $\Delta\kappa_\gamma$ and ΔQ_γ that are (1) gauge-fixing parameter (ξ) independent and (2) ultraviolet *and* infrared finite.

The paper is organized as follows. In Sec. II we review the S-matrix PT and discuss some of the more important results for our purposes. In addition, we briefly present the Degrassi-Sirlin alternative formulation of the PT. In Sec. III the S-matrix PT is used to construct the gauge-independent $\gamma W^+ W^-$ vertex with all incoming momenta

offshell, and explicit results are reported. Furthermore, we present a shortcut for deriving the gauge-independent vertex with the two W onshell *directly* from a process such as $e^+e^-\to W^+W^-$. In Sec. IV we prove the Ward identity that the gauge independent vertex satisfies. In Sec. V we calculate the functions $\hat{a}(Q^2)$ and evaluate numerically the pinch contributions to $\Delta\kappa_\gamma$ and ΔQ_γ. Finally, we summarize our results in Sec. VI.

II. THE PINCH TECHNIQUE

In this section we briefly review the S-matrix pinch technique (PT). In particular we outline the method of derivation of the gauge-independent proper self-energy of a gauge boson and comment on the technical differences that arise when PT is applied to a theory with symmetry breaking, such as the electroweak theory, as opposed to a theory such as QCD. In addition, we present the main idea of the Degrassi-Sirlin formulation of the PT, and establish some of the notation we will use in the sequel.

The S-matrix pinch technique is an algorithm that allows the construction of modified gauge-independent n-point functions, through the order by order resummation of Feynman graphs contributing to a certain physical and therefore ostensibly gauge-independent process (an S matrix in our case). The simplest example that demonstrates how the PT works is the gauge-boson two-point function (propagator). Consider the S-matrix element T for the elastic scattering of two fermions of masses M_1 and M_2. To any order in perturbation theory T is independent of the gauge fixing parameter ξ, defined by the free gluon propagator

$$\Delta_{\mu\nu}(q)=\frac{-g_{\mu\nu}+(1-\xi)(q_\mu q_\nu/q^2)}{q^2}\ . \tag{2.1}$$

On the other hand, as an explicit calculation shows, the conventionally defined proper self-energy [collectively depicted in Fig. 2(a)] depends on ξ. At the one-loop level

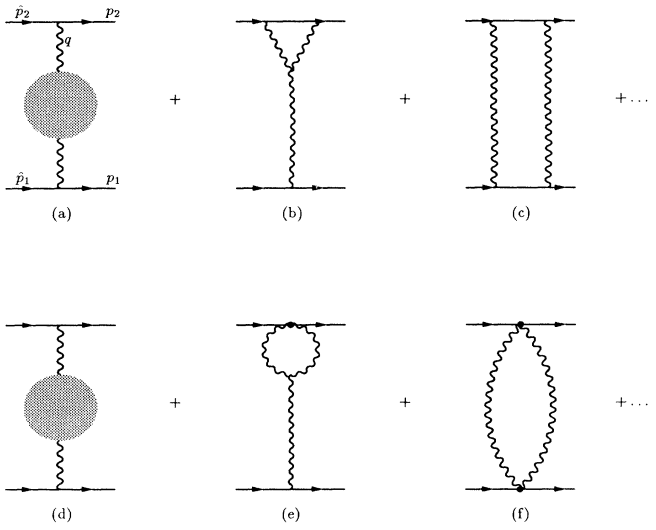

FIG. 2. Graphs (a)–(c) are some of the contributions to the S-matrix T. Graphs (e) and (f) are pinch parts, which, when added to the usual self-energy graphs (d), give rise to a gauge-independent effective self-energy.

this dependence is canceled by contributions from other graphs, such as Figs. 2(b) and 2(c), which do not seem to be of propagator type at first glance. That this must be so is evident from the form of T:

$$T(s,t,M_1,M_2)=T_1(t)+T_2(t,M_1,M_2)+T_3(s,t,M_1,M_2)\ , \tag{2.2}$$

where the function $T_1(t)$ depends only on the Mandelstam variable $t=-(\hat{p}_1-p_1)^2=-q^2$, and not on $s=(p_1+p_2)^2$ or on the external masses. The propagator-like parts of graphs such as Figs. 2(e) and 2(f), which enforce the gauge independence of $T_1(t)$, are called "pinch parts." The pinch parts emerge every time a gluon propagator or an elementary three-gluon vertex contribute a longitudinal k_μ to the original graph's numerator. The action of such a term is to trigger an elementary Ward identity of the form

$$\begin{aligned} k^\mu\gamma_\mu \equiv \not{k}&=(\not{p}+\not{k}-m)-(\not{p}-m)\\ &=S^{-1}(p+k)-S^{-1}(p) \end{aligned} \tag{2.3}$$

once it gets contracted with a γ matrix. The first term on the right-hand side of Eq. (2.3) will remove the internal fermion propagator, that is, a "pinch," whereas $S^{-1}(p)$ vanishes on shell. This last property characterizes the S-matrix PT we will use throughout this paper. Returning to the decomposition of Eq. (2.2), the function $T_1(t)$ is gauge invariant and unique and represents the contribution of the new propagator. We can construct the new propagator, or equivalently $T_1(t)$, directly from the Feynman rules. In doing so it is evident that any value for the gauge parameter ξ may be chosen, since T_1, T_2, and T_3 are all independent of ξ. The simplest of all covariant gauges is certainly the Feynman–'t Hooft gauge ($\xi=1$), which removes the longitudinal part of the gluon propagator. Therefore, the only possibility for pinching arises from the four-momentum of the three-gluon vertices, and the only propagatorlike contributions come from Fig. 2(b).

To explicitly calculate the pinching contribution of a graph such as Fig. 2(b) it is convenient to decompose the vertex in the following way, first proposed by 't Hooft. Group theory factors aside,

$$\Gamma_{\mu\nu\alpha}=\Gamma^P_{\mu\nu\alpha}+\Gamma^F_{\mu\nu\alpha} \tag{2.4}$$

with

$$\Gamma^P_{\mu\nu\alpha}\equiv(q+k)_\nu g_{\mu\alpha}+k_\mu g_{\nu\alpha} \tag{2.5}$$

and

$$\Gamma^F_{\mu\nu\alpha}\equiv 2q_\mu g_{\nu\alpha}-2q_\mu g_{\nu\alpha}-(2k+q)_\alpha q_{\mu\nu}\ . \tag{2.6}$$

$\Gamma^F_{\mu\nu\alpha}$ satisfies a Feynman-gauge Ward identity:

$$q^\alpha\Gamma^F_{\mu\nu\alpha}=[k^2-(k+q)^2]g_{\mu\nu}\ , \tag{2.7}$$

where the right-hand side (RHS) is the difference of two inverse propagators. As for $\Gamma^P_{\mu\nu\alpha}$ (P for "pinch") it gives rise to pinch parts when contracted with γ matrices

$$g_{\mu\alpha}(\not q+\not k)=g_{\mu\alpha}[(\not p+\not q-m)-(\not p-\not k-m)]$$
$$=g_{\mu\alpha}[S^{-1}(p+q)-S^{-1}(p-k)] \tag{2.8}$$

and

$$g_{\nu\alpha}\not k=g_{\nu\alpha}[(\not p-m)-(\not p-\not k-m)]$$
$$=g_{\nu\alpha}[S^{-1}(p)-S^{-1}(p-k)] \ . \tag{2.9}$$

Now both $S^{-1}(p+q)$ and $S^{-1}(p)$ vanish on shell, whereas the two terms proportional to $S^{-1}(p-k)$ pinch out the internal fermion propagator in Fig. 2(b). The total pinch contribution $\Pi^P(q)$ from Fig. 2(b) and its counterpart mirror image graph with the bubble attached to the bottom line is given by

$$\Pi^P(q)=(\tfrac{1}{2}N)\times 2\times 2\times\left[\frac{ig^2}{(2\pi)^4}\int\frac{d^4k}{k^2(k+q)^2}\right]$$
$$=-\frac{2Ng^2}{16\pi^2}\ln\left[\frac{-q^2}{\mu^2}\right], \tag{2.10}$$

where in the second equality we give the renormalized version of the integral. The factors in front of the integral are a group-theoretic factor $\frac{1}{2}N$ [N=number of colors in SU(N)]; one factor of 2 from the two pinching terms from Eqs. (2.8) and (2.9); another factor of 2 from the contribution of the mirror graph. In adding the pinch parts to the usual gluon self-energy one ambiguity needs resolution. Because we are working with the on-shell S matrix, any terms $\sim q_\mu q_\nu$ in the pinch parts do not show up in $T_1(t)$. We define uniquely the proper self-energy associated with the pinch parts by demanding that it be conserved [19]. So we define $\Pi^P_{\mu\nu}(q)$ as

$$\Pi^P_{\mu\nu}(q)=P_{\mu\nu}(q)\Pi^P(q) \ , \tag{2.11}$$

where

$$P_{\mu\nu}(q)\equiv -q^2 g_{\mu\nu}+q_\mu q_\nu \ . \tag{2.12}$$

Adding this to the usual Feynman-gauge proper self-energy

$$\Pi^{(\xi=1)}_{\mu\nu}(q)=\Pi^{(\xi=1)}(q)P_{\mu\nu}(q) \ , \tag{2.13}$$

with

$$\Pi^{(\xi=1)}(q)=-\frac{5}{3}N\frac{g^2}{16\pi^2}\ln\left[\frac{-q^2}{\mu^2}\right], \tag{2.14}$$

we find for $\hat{\Pi}_{\mu\nu}(q)$ the gauge invariant combination

$$\hat{\Pi}_{\mu\nu}(q)=P_{\mu\nu}(q)\hat{\Pi}(q) \ , \tag{2.15}$$

with

$$\hat{\Pi}(q)=-bg^2\ln\left[\frac{-q^2}{\mu^2}\right] \tag{2.16}$$

and

$$b=\frac{11N}{48\pi^2} \tag{2.17}$$

the coefficient of $-g^3$ in the usual one loop β function. Finally, the full modified propagator $\hat{\Delta}_{\mu\nu}(q)$ at one-loop order reads

$$\hat{\Delta}_{\mu\nu}(q)=P_{\mu\nu}(q)\hat{d}(q)-\xi\frac{q_\mu q_\nu}{q^4} \ , \tag{2.18}$$

with

$$\hat{d}^{-1}(q)=1-\hat{\Pi}(q)$$
$$=1+bg^2\ln\left[\frac{-q^2}{\mu^2}\right]. \tag{2.19}$$

We see that the modified propagator has a gauge independent self-energy and only a trivial gauge dependence originating from the tree part given by Eq. (21).

It is important to emphasize at this point that the gauge-invariant self-energies and vertices obtained by the application of the S-matrix pinch technique do *not* depend on the particular process employed (fermion + fermion → fermion + fermion, fermion + fermion → gluon + gluon, gluon + gluon → gluon + gluon, etc.) and are in that sense universal. This fact can be seen with an explicit calculation, where one can be convinced that the only quantities entering in the definition of the gauge-independent self-energies and vertices are just the gauge group structure constants, and that the only difference from process to process is the external group matrices associated with external-leg wave functions, due to the different particle assignments, which are, of course, immaterial to the definition of the things inside. A very instructive example of an explicit calculation, where two different processes give rise to *exactly* the same self-energy for the W gauge boson, is given in [17].

Finally, we conclude this section with a brief presentation of an alternative formulation of the PT introduced in [17] in the context of the standard model. In this approach the interaction of gauge bosons with external fermions is expressed in terms of current correlation functions, i.e., matrix elements of Fourier transforms of time-ordered products of current operators [20]. This is particularly economical because these amplitudes automatically include several closely related Feynman diagrams. When one of the current operators is contracted with the appropriate four-momentum, a Ward identity is triggered. The pinch part is then identified with the contributions involving the equal-time commutators in the Ward identities, and therefore involve amplitudes in which the number of current operators has been decreased by one or more. A basic ingredient in this formulation are the following equal-time commutators, some of which we will also employ later in Sec. III:

$$\delta(x_0-y_0)[J^0_W(x),J^\mu_W(y)]=c^2J^\mu_W(x)\delta^4(x-y) \ , \tag{2.20}$$

$$\delta(x_0-y_0)[J^0_W(x),J^{\mu\dagger}_W(y)]=-J^\mu_3(x)\delta^4(x-y) \ , \tag{2.21}$$

$$\delta(x_0-y_0)[J^0_W(x),J^\mu_\gamma(y)]=J^\mu_W(x)\delta^4(x-y) \ , \tag{2.22}$$

with $J^\mu_3\equiv 2(J^\mu_Z+s^2J^\mu_\gamma)$. On the other hand,

$$\delta(x_0-y_0)[J^0_V(x),J^\mu_{V'}(y)]=0 \ , \tag{2.23}$$

where $V,V'\in\{\gamma,Z\}$. To demonstrate the method with

an example, consider the vertex Γ_μ shown in Fig. 2(b), where now the gauge particles in the loop are W's instead of gluons and the incoming and outgoing fermions are massless. It can be written (with $\xi=1$)

$$\Gamma_\mu=\int\frac{d^4k}{2\pi^4}\Gamma_{\mu\alpha\beta}(q,k,-k-q)\times\int d^4x e^{ikx}\langle f|T^*[J_W^{\alpha\dagger}(x)J_W^{\beta}(0)]|i\rangle\ . \quad (2.24)$$

When an appropriate momentum, say k_α, from the vertex is pushed into the integral over dx, it gets transformed into a covariant derivative d/dx_α acting on the time-ordered product $\langle f|T^*[J_W^{\alpha\dagger}(x)J_W^{\beta}(0)]|i\rangle$. After using current conservation and differentiating the θ-function terms, implicit in the definition of the T^* product, we end up with the left-hand side of Eq. (2.21). So, the contribution of each such term is proportional to the matrix element of a single current operator, namely $\langle f|J_3^\mu|i\rangle$; that is precisely the pinch part. Calling Γ_μ^P the total pinch contribution from the Γ_μ of Eq. (2.24), we find that

$$\Gamma_\mu^P=-g^3cI_{WW}(Q^2)\langle f|J_3^\mu|i\rangle\ , \quad (2.25)$$

where

$$I_{ij}(q)=i\int\left[\frac{d^4k}{2\pi^4}\right]\frac{1}{(k^2-M_i^2)[(k+q)^2-M_j^2]}\ . \quad (2.26)$$

Obviously, the integral in Eq. (2.26) is the generalization of the QCD expression Eq. (2.10) to the case of massive gauge bosons.

III. THE GAUGE-INVARIANT THREE-VECTOR-BOSON VERTICES

After this brief introduction to the PT, we now focus on the main topic of this paper. In this section we use the S-matrix PT to construct at one-loop order gauge-independent three-boson vertices in the context of the standard model, when *all* incoming momenta are off shell. This problem has first been addressed in the case of QCD in [13]. The generalization of the method to the case of the standard model was outlined in [17] and the general structure of the new vertices was derived; however no explicit expressions for the pinch contributions were reported. Since these contributions are essential for rendering the final expressions of the static properties of the W bosons gauge-independent and infrared finite, we will record in this section their explicit expressions.

We consider the S-matrix element for the process $e^+e^-\to e^+\bar{\nu}_e e^-\nu_e$. Without any loss of generality we will consider all external fermions to be massless [21]. The loop diagrams contributing to the S matrix can be classified in several distinct classes: vector-boson-vertex diagrams (such as in Figs. 4 and 5), vector-boson self-energy diagrams (Fig. 9), fermion-fermion-boson-vertex diagrams [Fig. 6(c)], and boxlike diagrams [Figs. 6(a), 7(a), and 8(a)]. In addition, there are propagator corrections to the external fermions as well as disconnected graphs, which are clearly irrelevant for our purposes, and we therefore omit them. We can extract a gauge-independent improper vertex by identifying the part $\hat{T}(q,p_1,p_2)$ of the S matrix which is independent of the external momenta l_i and $\hat{l}_i$, and depends only on the momentum transfers q,p_1,p_2. The general form of $\hat{T}(q,p_1,p_2)$ is shown in Fig. 3. It is ξ independent as long as we add all Feynman graphs *and* parts of Feynman graphs that depend only on the momentum transfers q,p_1,p_2. So, to the usual vertex-diagrams we must add the vertexlike contributions extracted from the boxlike graphs, as shown schematically in Figs. 6–8 and their mirror image graphs. The inclusion of these extra pieces gives rise to a gauge-independent expression for $\hat{T}(q,p_1,p_2)$. Before we record our results a few technical remarks are warranted. The sum of all contributions mentioned above assumes the form of an improper vertex, namely,

$$\hat{T}(q,p_1,p_2)\equiv\hat{\Delta}(q)\hat{\Delta}(p_1)\hat{\Delta}(p_2)\hat{\Gamma}(q,p_1,p_2)\ , \quad (3.1)$$

"sandwiched" between external spinors, not explicitly shown. The propagators $\hat{\Delta}$ in Eq. (3.1) are those constructed via the PT according to [17]; they have gauge-independent self-energies and only a trivial gauge dependence, namely that of their tree-level form. This trivial gauge dependence of all the $\hat{\Delta}$ does not appear in $\hat{T}(q,p_1,p_2)$, since the external fermions are on shell and massless. Therefore, we can recover the gauge-independent proper $\hat{\Gamma}(q,p_1,p_2)$ from $\hat{T}(q,p_1,p_2)$, by stripping off the $\hat{\Delta}$'s, as if they had no longitudinal pieces at all. Another equivalent and more economical way to isolate the proper vertex (as described in [13] and [17]) is to notice that the gauge boson self-energies can be converted to gauge-independent ones through PT, up to a missing piece, namely the pinch contribution of the mirror graph of Fig. 2(e), which clearly is not present in the process we consider. The missing piece may be added by hand to $\hat{\Delta}$, and then subtracted from $\hat{\Gamma}$. So, the proper vertex emerges if we neglect all gauge boson self-energy corrections and subtract instead half of the self-energy

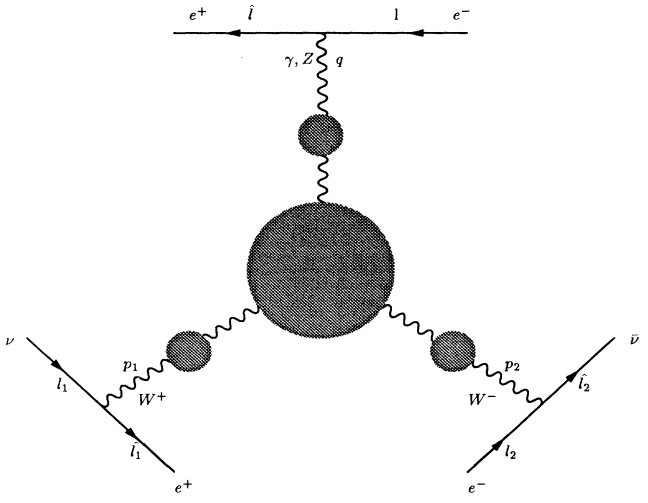

FIG. 3. The general structure of the part $T(q,p_1,p^2)$ of the S matrix, that only depends on the momentum transfers.

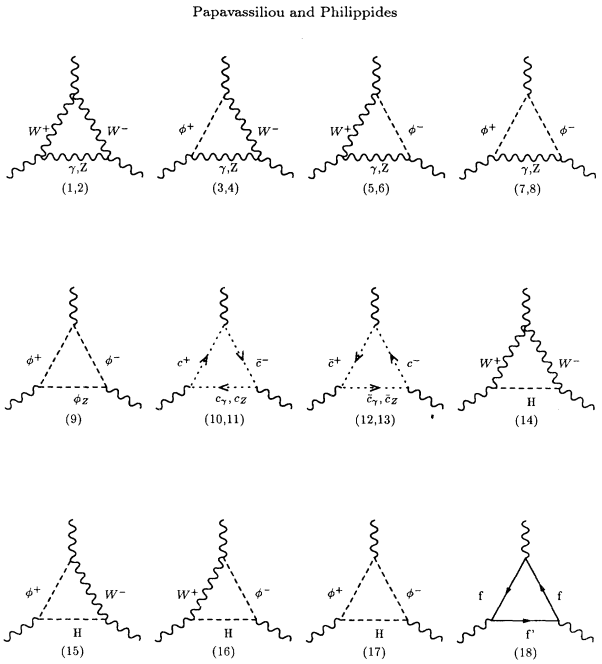

FIG. 4. The usual triangle graphs contributing to the γW^+W^- vertex, referred to as $V^i_{\mu\alpha\beta}$ in the text. All graphs are understood to be sandwiched between external fermions, as in Fig. 3.

pinch contribution for each leg.

We now turn to the details of the calculation. Since the final result, when correctly constructed, is *ostensibly* gauge independent, we are allowed to perform the calculation in *any gauge. We choose the Feynman–'t Hooft gauge* ($\xi_i=1$, with $i=\gamma,Z,W$), since it is certainly the most convenient one. As we already explained, in this gauge pinching terms arise only from diagrams that contain elementary three-vector-boson vertices. We will use the following notation: Scalar propagators are generally denoted as

$$D_i(p)=\frac{1}{p^2-M_i^2}\ . \tag{3.2}$$

The trilinear vertex at tree level is given by

$$\Gamma_{\alpha\beta\gamma}(k_1,k_2,k_3)=g_{\alpha\beta}(k_1-k_2)_\gamma+g_{\beta\gamma}(k_2-k_3)+g_{\gamma\alpha}(k_3-k_1)_\beta\ . \tag{3.3}$$

Left and right projectors are defined as

$$P_{R,L}=\tfrac{1}{2}(1\pm\gamma_5)\ . \tag{3.4}$$

We denote by $(dk)\equiv d^4k/i(2\pi)^4$ the loop integration measure for convergent integrals and by $(dk)\equiv\mu^{4-n}[d^nk/i(2\pi)^n]$ the measure for divergent ones, with μ the 't Hooft mass scale of dimensional regularization.

To construct the gauge-independent vertex, we add to the regular vertex graphs of Figs. 4 and 5 (which we will call $V^i_{\mu\alpha\beta}$) the vertexlike pinch parts that arise from the box diagrams shown in Figs. 6(b), 7(b), and 8(c). Clearly,

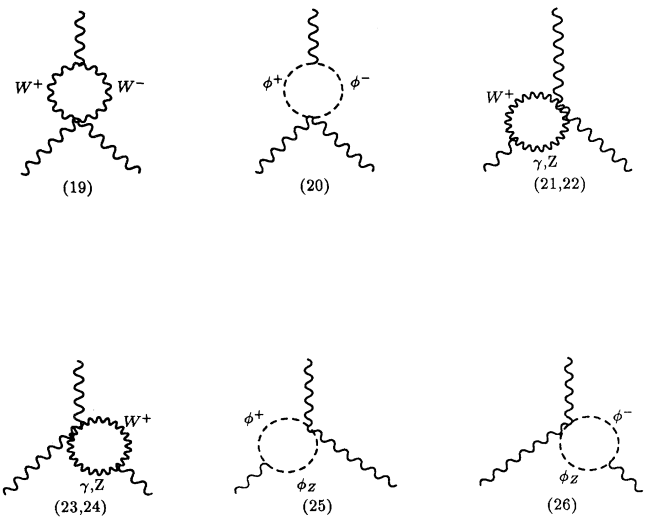

FIG. 5. The rest of the usual $V^i_{\mu\alpha\beta}$ graphs contributing to the γW^+W^- vertex.

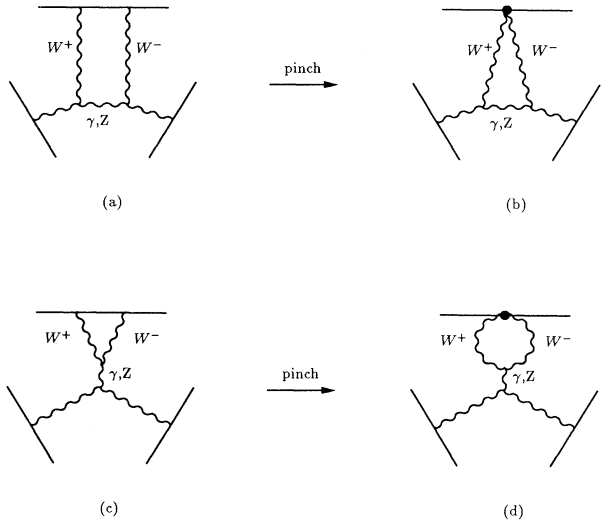

FIG. 6. Graphs (a) and (c) contribute to the gauge-independent vertex through their pinch parts, graphs (b) and (d), respectively. Notice the absence of box graphs containing $\gamma\gamma$, ZZ, or $Z\gamma$ legs.

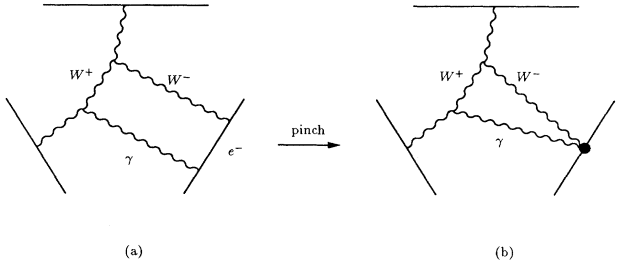

FIG. 7. The pinch contribution of the box containing a γ.

we must also include the mirror graphs corresponding to Figs. 7(b) and 8(c) which are hooked on the external fermions of the left-hand side, and are not shown explicitly. To begin with, from the box diagrams of the type shown in Fig. 6(a), only those with two W's in the loop will contribute a vertexlike pinch part. The rest contain two neutral gauge vector bosons ($\gamma\gamma,\gamma Z,Z\gamma,ZZ$) and, unlike Fig. 6(a), they also have crossed graphs, the pinch part of which cancels the pinch part of the direct diagrams. This is most easily seen in the framework of the PT formulation of [17]; since the equal-time commutator of the relevant currents J_γ,J_Z is zero [see Eq. (2.23)], their total pinch contribution vanishes.

The total pinch contribution of Fig. 6(a) is proportional to $g^2\gamma^\mu P_L$ and can be written as linear combination of J^μ_γ and J^μ_Z, namely $g^2\gamma^\mu P_L=\frac{1}{2}(s^2J^\mu_\gamma+J^\mu_Z)$. The first term will be allotted to the γWW vertex and the second to the ZWW vertex. If we define

$$B_{\mu\alpha\beta}(q,p_1,p_2)=\sum_V g_V^2 B^V_{\mu\alpha\beta}(q,p_1,p_2)\ , \tag{3.5}$$

where $B^V_{\mu\alpha\beta}$ is the integral

$$B^i_{\mu\alpha\beta}(q,p_1,p_2)=\int(dk)D_i(k)D_W(k+p_1)D_W(k-p_2)\{g_{\mu\alpha}(2p_{1\beta}-3k_\beta)+g_{\alpha\beta}[k_\mu-\tfrac{3}{2}(p_1-p_2)_\mu]-g_{\mu\beta}(2p_{2\alpha}+3k_\alpha)\} \tag{3.6}$$

and the summation index $V=\gamma,Z$ refers to the *internal* γ or Z propagator, then the pinch contribution of these box diagrams is

$$[\text{Fig. 6(b)}]_{\gamma WW}=(-gs)q^2B_{\mu\alpha\beta}(q,p_1,p_2) \tag{3.7}$$

and

$$[\text{Fig. 6(b)}]_{ZWW}=(-gc)[q^2-M_Z^2]B_{\mu\alpha\beta}(q,p_1,p_2) \tag{3.8}$$

for the γWW and ZWW vertices, respectively.

We next look at the pinch contributions of the box diagrams of the type shown in Figs. 7 and 8. There are two such contributions, depending on whether the pinching occurs at the side of the W^+ or at the side of the W^- [the latter are shown in Figs. 7(b) and 8(c)]. We call them, respectively, $B^+_{\mu\alpha\beta}$ and $B^-_{\mu\alpha\beta}$ and they are connected by the relation

$$B^-_{\mu\alpha\beta}(q,p_1,p_2)=-B^+_{\mu\beta\alpha}(q,p_2,p_1)\ . \tag{3.9}$$

It is clear from Fig. 8 that when the neutral vector boson in the loop is a Z, we have a direct and a crossed graph. These two graphs are different, since the internal fermion is an e or a ν, respectively. The pinch parts of the direct and crossed diagram are again opposite to each other, but since the couplings are different, their total sum is not zero, according to $(\nu We)(eZe)-(\nu Z\nu)(\nu We)=-g_Z(\nu We)$.

Then $B^+_{\mu\alpha\beta}$ is given by

$$B^+_{\mu\alpha\beta}(q,p_1,p_2)=\sum_V g_V^2 G^V_{\mu\alpha\beta}(q,p_1,p_2) \tag{3.10}$$

where $G^V_{\mu\alpha\beta}$ is the integral

$$G^V_{\mu\alpha\beta}(q,p_1,p_2)=\int(dk)D_V(k)D_W(k+p_1)D_W(k-p_2)[g_{\alpha\beta}(3k+2p_1-3p_2)_\mu+g_{\beta\mu}(-k+4p_2)_\alpha+g_{\alpha\mu}(3k-2p_1)_\beta] \tag{3.11}$$

and V is again summed over the internal γ and Z propagator. Finally, the pinch parts of the box diagrams of this type are

$$[\text{Fig. 7(b)}]+[\text{Fig. 8(c)}]=-g_V(p_2^2-M_W^2)B^-_{\mu\alpha\beta}\ , \tag{3.12}$$

$$[\text{mirror image of Fig. 7(b)}]+[\text{mirror image of Fig. 8(c)}]=-g_V(p_1^2-M_W^2)B^+_{\mu\alpha\beta}\ , \tag{3.13}$$

where g_V is equal to gs or gc depending on which gauge-independent vertex (γW^+W^- or ZW^+W^-) we consider. Notice the presence of the typical inverse-propagatorlike factor $D_W^{-1}(p_1)=p_1^2-M_W^2$, which always multiplies expressions originating from pinching. Before we proceed, we record the result of q^μ acting on $G^V_{\mu\alpha\beta}$ of Eq. (3.11), which will be used in the next section:

$$q^\mu G^V_{\mu\alpha\beta}=2g_{\alpha\beta}[I_{VW}(p_1)-I_{VW}(p_2)]+\int(dk)D_V(k)D_W(k+p_1)D_W(k-p_2)[q_\alpha k_\beta+q^\rho\Gamma_{\rho\alpha\beta}(-p_2+k,-k,p_2)]\ , \tag{3.14}$$

where $I_{ij}(p)$ has been defined in Eq. (2.26).

As we already explained at the beginning of this section, in order to isolate the proper vertex we must subtract half of the contribution of the self-energy pinch graphs for the propagator of each leg. All such contributions are of the general form

$$\Gamma_{\mu\alpha\beta}(q,p_1,p_2)I_{JW}(p)\ , \tag{3.15}$$

where $J=W,\gamma,Z$ and $p=q,p_1,p_2$, $\Gamma_{\mu\alpha\beta}$ is the tree-level γW^+W^- or ZW^+W^- vertex [Fig. 6(d)]. We will not reproduce the details of this last step here. (See [17] for more details.)

Finally, the one-loop gauge-independent trilinear gauge boson vertices (after we pull out a factor of $-igc$ or $-igs$) are

$$\hat{\Gamma}_{\mu\alpha\beta}=V_{\mu\alpha\beta}-(q^2-M_V^2)B_{\mu\alpha\beta}-(p_1^2-M_W^2)B^+_{\mu\alpha\beta}-(p_1^2-M_W^2)B^-_{\mu\alpha\beta}-2g^2\Gamma_{\mu\alpha\beta}[I_{WW}(q)+s^2I_{\gamma W}(p_1)+c^2I_{ZW}(p_1)+s^2I_{\gamma W}(p_2)+c^2I_{ZW}(p_2)]\ , \tag{3.16}$$

where $V_{\mu\alpha\beta}=\sum_i V^i_{\mu\alpha\beta}$ are the usual one-loop corrections to the γW^+W^- or ZW^+W^- vertex in the Feynman gauge ($\xi_i=1, i=\gamma,Z,W$). The one-loop diagrams of the γWW vertex in this gauge are shown in Figs. 4 and 5. There are a few additional graphs for the ZW^+W^- vertex, due to the tree level coupling of Z to the Higgs boson.

The vertex constructed via the S-matrix PT in the way we described above represents the most general case, since all three incoming momenta are off shell. If one is interested in the simpler case, where the two incoming momenta of W^+ and W^- are on shell, and only the photon momentum is off shell, as is the case, for example, in the process $e^+e^-\to W^+W^-$, Eq. (3.16) reduces to the expression

$$\hat{\Gamma}_{\mu\alpha\beta}\big|_{p_1^2=p_2^2=M_W^2}=V_{\mu\alpha\beta}-(q^2-M_V^2)B_{\mu\alpha\beta}-2g^2\Gamma_{\mu\alpha\beta}I_{WW}(q)\ . \tag{3.17}$$

This is of course the same answer one obtains by applying the PT *directly* to the S matrix of $e^+e^-\to W^+W^-$. Clearly, in that case the only vertexlike contribution comes from graph Fig. 6(a), and is just $g_V B_{\mu\alpha\beta}q^2$, whereas the term $-2g_Vg^2\Gamma_{\mu\alpha\beta}I_{WW}(q)$ arises exactly as before, namely as a leftover from the construction of gauge independent $\gamma\gamma,\gamma Z$, and ZZ self-energies. We note that with the two W's on shell the $B_{\mu\alpha\beta}$ function becomes infrared divergent. This divergence, however, cancels against the infrared divergences that the $V^1_{\mu\alpha\beta}$ diagram develops as well, when the two W's are considered on shell. This will be shown in Sec. V.

IV. THE WARD IDENTITY FOR THE γWW VERTEX

In this section we show that the one-loop gauge-invariant γWW vertex $\hat{\Gamma}_{\mu\alpha\beta}$ constructed in the previous section via the S-matrix PT satisfies a simple QED-like Ward identity, which relates it to the gauge-invariant one-loop self-energy $\hat{\Pi}_{\alpha\beta}$ of the W, constructed in [17] [Eq. (19)].

The proof of the Ward identity is rather lengthy and technically involved; we therefore start this section by recording the result, for the reader who wants a quick tour through the paper. The gauge-invariant γW^+W^- vertex $\hat{\Gamma}_{\mu\alpha\beta}(q,p_1,p_2)$ and the gauge-invariant W self-energy $\hat{\Pi}_{\alpha\beta}$ satisfy the Ward identity

$$q^\mu\hat{\Gamma}_{\mu\alpha\beta}(q,p_1,p_2)=\hat{\Pi}_{\alpha\beta}(p_1^2)-\hat{\Pi}_{\alpha\beta}(p_2^2)\ , \tag{4.1}$$

with

$$\hat{\Pi}_{\alpha\beta}(p^2)=\Pi_{\alpha\beta}(p^2)-4g^2(p^2-M_W^2)[c^2I_{ZW}(p^2)+s^2I_{\gamma W}(p^2)]\ , \tag{4.2}$$

where $\Pi_{\alpha\beta}(p)$ are the usual one-loop W self-energy contributions with tadpole contributions incorporated, in the Feynman gauge. The second term is the pinch part, which is given diagrammatically in Fig. 9 (pinch).

We now proceed to prove Eq. (4.1). In doing so, we find it more economical to act with q_μ *directly* on the Feynman graphs, instead of first evaluating them and then act with q_μ on the final answer. In this way, cancellations among entire graphs become immediately apparent. The W self-energy diagrams that are relevant for the construction of the RHS of Eq. (4.1) are shown in Fig. 9. Seagull and tadpole diagrams are omitted, since they do not depend on the momenta p_1 or p_2, and thus cancel when we form the difference of the two self-energies in Eq. (4.1).

We now contract the RHS of Eq. (3.16) with q^μ. The following identity is frequently used:

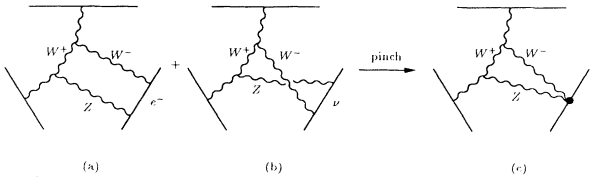

FIG. 8. The pinch contribution of the box containing a Z. notice that the direct and the crossed graphs are not equivalent, since the internal fermion is an electron or a neutrino, respectively.

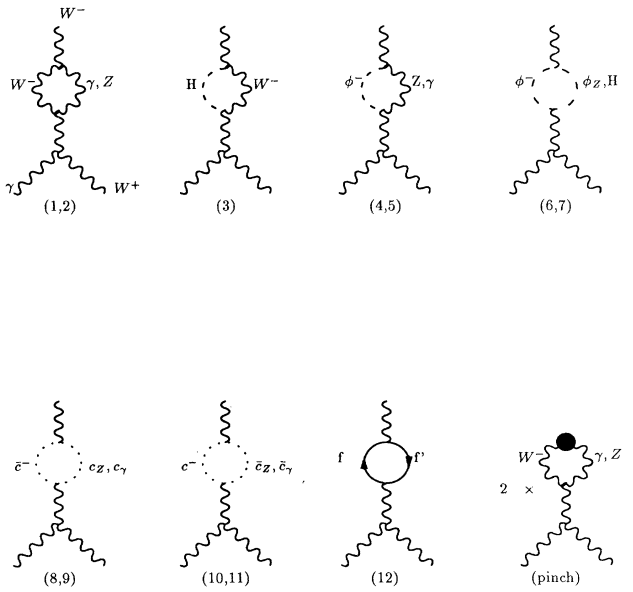

FIG. 9. The Feynman graphs contributing to the gauge-independent WW self-energy. The last graph denotes the pinch contributions (in the $\xi=1$ gauge).

$$k_2^{\beta}\Gamma_{\alpha\beta\gamma}(k_1,k_2,k_3)=P_{\alpha\gamma}(k_1)-P_{\alpha\gamma}(k_3)$$
$$=g_{\alpha\gamma}[D_i^{-1}(k_1)-D_j^{-1}(k_3)]-k_{1\alpha}k_{1\gamma}+k_{3\alpha}k_{3\gamma}+g_{\alpha\gamma}\Delta M_{ij}^2 , \tag{4.3}$$

with $\Delta M_{ij}^2=M_i^2-M_j^2$.

We start with the vertex pinch parts $B^{+}_{\mu\alpha\beta}$, $B^{-}_{\mu\alpha\beta}$, and $B_{\mu\alpha\beta}$; using Eq. (3.14) we obtain

$$-q^{\mu}B^{+}_{\mu\alpha\beta}D_W^{-1}(p_1)=-D_W^{-1}(p_1)\sum_V g_V^2\left[2g_{\alpha\beta}[I_{VW}(p_1)-I_{VW}(p_2)]+\int(dk)D_V(k)D_W(k+p_1)D_W(k-p_2)\right.$$
$$\left.\times[q_{\alpha}k_{\beta}+q^{\rho}\Gamma_{\rho\alpha\beta}(-p_2+k,-k,p_2)]\right] \tag{4.4}$$

and

$$-q^{\mu}B^{-}_{\mu\alpha\beta}D_W^{-1}(p_2)=-D_W^{-1}(p_2)\sum_V g_V^2\left[2g_{\alpha\beta}[I_{VW}(p_1)-I_{VW}(p_2)]+\int(dk)D_V(k)D_W(k+p_1)D_W(k-p_2)\right.$$
$$\left.\times[q_{\beta}k_{\alpha}+q^{\rho}\Gamma_{\rho\alpha\beta}(-p_1-k,p_1,k)]\right] . \tag{4.5}$$

On the other hand $q^{\mu}B_{\mu\alpha\beta}=0$, since the J^{μ}_{γ} current is divergenceless.

We continue with the self-energy pinch parts of the vertex; using Eq. (4.3), we get

$$-2g^2g_{\alpha\beta}[D_W^{-1}(p_2)-D_W^{-1}(p_1)][I_{WW}(q^2)+s^2I_{\gamma W}(p_1^2)+c^2I_{ZW}(p_1^2)+s^2I_{\gamma W}(p_2^2)+c^2I_{ZW}(p_2^2)] , \tag{4.6}$$

where terms proportional to $p_{1\alpha}$ or $p_{2\beta}$, that are zero on shell, have been discarded [19].

The first terms of Eqs. (4.4) and (4.5) when combined with the last four terms of Eq. (4.6) give

$$\sum_V 2g_V^2g_{\alpha\beta}\{[D_W^{-1}(p_1)+D_W^{-1}(p_2)][I_{VW}(p_1)-I_{VW}(p_2)]-[D_W^{-1}(p_2)-D_W^{-1}(p_1)][I_{VW}(p_1)+I_{VW}(p_2)]\}$$
$$=\sum_V 4g_V^2g_{\alpha\beta}\{D_W^{-1}(p_1)I_{VW}(p_1)-D_W^{-1}(p_2)I_{VW}(p_2)\} . \tag{4.7}$$

We recognize in this last term the difference of the pinch contributions that render the W self-energies, defined at p_1 and p_2, gauge independent.

We continue by calculating the divergence of the diagrams of Fig. 4 (1,2) $V^1_{\mu\alpha\beta}$ and $V^2_{\mu\alpha\beta}$, given by

$$V^{1,2}=-g_V^2\int(dk)D_V(k)D_W(k+p_1)D_W(k-p_2)$$
$$\times\Gamma_{\mu\rho\sigma}(q,p_1+k,p_2-k)\Gamma^{\rho}_{\alpha\lambda}(p_1,k,-p_1-k)\Gamma^{\sigma\lambda}_{\beta}(p_2,k-p_2,-k) . \tag{4.8}$$

When contracting the expression above with q^{μ} the identity Eq. (4.3) is triggered and we get

$$q^{\mu}V^{1,2}_{\mu\alpha\beta}=-g_V^2\int(dk)D_V(k)D_W(k+p_1)D_W(k-p_2)\Gamma^{\rho}_{\alpha\lambda}(p_1,k,-p_1-k)\Gamma^{\sigma\lambda}_{\beta}(p_2,k-p_2,-k)$$
$$\times\{g_{\rho\sigma}[D_W^{-1}(p_2-k)-D_W^{-1}(p_1-k)]+(p_1+k)_{\rho}(p_1+k)_{\sigma}-(p_2-k)_{\rho}(p_2-k)_{\sigma}\} . \tag{4.9}$$

We first concentrate on the $g_{\rho\sigma}$ term. It reads

$$-g_V^2\int(dk)[D_V(k)D_W(k+p_1)-D_V(k)D_W(k-p_2)]\Gamma_{\alpha\lambda\sigma}(p_1,k,-p_1-k)\Gamma^{\sigma\lambda}_{\beta}(p_2,k-p_2,-k) . \tag{4.10}$$

It contains only two internal propagators and could be identified with the self-energy graphs $\Pi^{1,2}_{\alpha\beta}$ of Fig. 9 (1,2) *if* the $\Gamma_{\alpha\lambda\sigma}\Gamma^{\sigma\lambda}{}_{\beta}$ factor had the appropriate momenta arguments. To convert this term to the desired form, we use $p_1+p_2+q=0$ to write

$$\Gamma^{\sigma\lambda}{}_{\beta}(k-p_2,-k,p_2)=\Gamma^{\sigma\lambda}{}_{\beta}(k+p_1,-k,-p_1)+2q^{\lambda}g^{\sigma}_{\beta}-q^{\sigma}g^{\lambda}{}_{\beta}-q_{\beta}g^{\sigma\lambda} \tag{4.11}$$

for the first part, and

$$\Gamma_{\alpha\lambda\sigma}(p_1,k,-p_1-k)=\Gamma_{\alpha\lambda\sigma}(p_2-k,-p_2,k)+2q_{\lambda}g^{\rho}_{\alpha}-q^{\rho}g_{\alpha\lambda}-q_{\alpha}g^{\rho}_{\lambda} \tag{4.12}$$

for the second part. After bringing the Γ's in the correct form, we recognize that the terms leftover in Eqs. (4.11) and (4.12) are equal to $-\sum_i q^{\mu}V^i_{\mu\alpha\beta}$ for $i=21, 22, 23, 24$, namely the negative of the divergence of the diagrams in Fig. 5 (21, 22, 23, 24); thus all these contributions will cancel in the left-hand side of Eq. (4.1).

So, the term proportional to $g_{\rho\sigma}$ is equal to

$$-[\Pi^{1,2}_{\alpha\beta}(p_2)-\Pi^{1,2}_{\alpha\beta}(p_2)]-q^\mu V^{21,20}_{\mu\alpha\beta}-q^\mu V^{23,22}_{\mu\alpha\beta} \ . \tag{4.13}$$

We next examine the term $(p_1+k)_\rho(p_1+k)_\sigma-(p_2-k)_\rho(p_2-k)_\sigma$ of Eq. (4.9). Contracting each momentum of this term with the appropriate vertex in order to exploit Eq. (4.3), we obtain

$$g_V^2\int(dk)D_V(k)D_W(k+p_1)D_W(k-p_2)[q^\rho\Gamma_{\rho\lambda\beta}(k-p_2,-k,p_2)\{[D_W^{-1}(p_1)-D_V^{-1}(k)]g_\alpha^\lambda+\Delta M^2_{WV}g_\alpha^\lambda+k_\alpha k^\lambda\}$$
$$+q^\rho\Gamma_{\alpha\lambda\rho}(p_1,k,-p_1-k)\{[D_W^{-1}(p_2)-D_V^{-1}(k)]g_\beta^\lambda+\Delta M^2_{WV}g_\beta^\lambda+k_\beta k^\lambda\}] \ , \tag{4.14}$$

where we have omitted terms proportional to $p_{1\alpha}$ or $p_{2\beta}$ that are zero on shell. Using the identity

$$-eg_V^2\Delta M^2_{WV}=-b_V g^3\sin^3\theta M_W^2 \ , \tag{4.15}$$

where $b_\gamma=+1$ and $b_Z=-1$, we recognize that the terms of Eq. (4.14) proportional to ΔM^2_{WV} are equal to $-\sum_i q^\mu V^i_{\mu\alpha\beta}$ of Fig. 4 (3, 4, 5, 6); all these contributions will also cancel in Eq. (4.1).

We continue by noticing that in the $D_V^{-1}(k)$ terms of Eq. (4.14) the $V=\gamma,Z$ propagators cancel, and the resulting expression depend on V only through the coupling g_V^2, namely

$$-g_V^2\int(dk)D_W(k+p_1)D_W(k-p_2)$$
$$\times q^\rho\Gamma_{\rho\alpha\beta}(q,p_1-k,p_2+k) \ . \tag{4.16}$$

So, when we add the diagrams of Fig. 4(1,2), the couplings will give $-g^2$, and after using Eq. (4.3) in Eq. (4.16), and shifting the integration variables, we get, for this last term,

$$=g^2\int(dk)D_W(p_1+k)D_W(p_2-k)(4q\cdot k)g_{\alpha\beta}$$
$$=2g^2g_{\alpha\beta}[D_W^{-1}(p_2)-D_W^{-1}(p_1)]I_{WW}(q) \tag{4.17}$$

which will cancel against the first term of Eq. (4.6).

For the $k_\alpha k^\lambda$ and $k_\beta k^\lambda$ terms of Eq. (4.14) we perform the contractions $k^\lambda\Gamma_{\rho\lambda\beta}$ and $k^\lambda\Gamma_{\rho\alpha\lambda}$, and we get

$$=g_V^2\int(dk)D_V(k)D_W(k+p_1)D_W(k-p_2)$$
$$\times[k_\alpha q_\beta D_W^{-1}(p_2)+k_\beta q_\alpha D_W^{-1}(p_1)+q(k-p_2)k_\alpha k_\beta$$
$$+q(k+p_1)k_\alpha k_\beta] \tag{4.18}$$

and terms that are zero on shell have been omitted. Collecting the terms proportional to $D_W^{-1}(p_1)$ and $D_W^{-1}(p_2)$ from the above equation and from Eq. (4.14), we immediately see that they cancel against the second terms of Eqs. (4.4) and (4.5). It is now important to recognize that the two remaining terms of Eq. (4.18) are equal to the divergence of the vertex diagrams containing a ghost loop [Fig. 4, diagrams (10, 11, 12, 13)], and their presence is crucial for recovering the W self-energies on the RHS of Eq. (4.1). Indeed, from the vertex graphs with ghosts we obtain

$$q^\mu(V^{10}_{\mu\alpha\beta}+V^{12}_{\mu\alpha\beta})=\Pi^8_{\alpha\beta}(p_1)-\Pi^8_{\alpha\beta}(p_2) \tag{4.19}$$

and

$$q^\mu(V^{11}_{\mu\alpha\beta}+V^{13}_{\mu\alpha\beta})=\Pi^9_{\alpha\beta}(p_1)-\Pi^9_{\alpha\beta}(p_2) \ , \tag{4.20}$$

where the diagrams

$$\Pi^9_{\alpha\beta}=\Pi^{11}_{\alpha\beta} \ , \quad \Pi^8_{\alpha\beta}=\Pi^{10}_{\alpha\beta} \tag{4.21}$$

are the ghost one-loop corrections to the W self-energy, and are shown in Fig. 9 (8, 9, 10, 11). Evidently, the vertex ghost diagrams contribute *only* half of the necessary self-energy ghost diagrams, while the other half will be provided by the last two terms of Eq. (4.18).

In a straightforward way we also arrive at the following results.

Higgs diagrams

$$q^\mu V^{14}_{\mu\alpha\beta}=\Pi^3_{\alpha\beta}(p_1)-\Pi^3_{\alpha\beta}(p_2)-q^\mu V^{15}_{\mu\alpha\beta}-q^\mu V^{16}_{\mu\alpha\beta} \ , \tag{4.22}$$

$$q^\mu V^{17}_{\mu\alpha\beta}=\Pi^6_{\alpha\beta}(p_1)-\Pi^6_{\alpha\beta}(p_2) \ . \tag{4.23}$$

Goldstone boson diagrams

$$q^\mu V^7_{\mu\alpha\beta}=\Pi^5_{\alpha\beta}(p_1)-\Pi^5_{\alpha\beta}(p_2) \ , \tag{4.24}$$

$$q^\mu V^8_{\mu\alpha\beta}=\Pi^4_{\alpha\beta}(p_1)-\Pi^4_{\alpha\beta}(p_2) \ , \tag{4.25}$$

$$q^\mu V^9_{\mu\alpha\beta}=\Pi^7_{\alpha\beta}(p_1)-\Pi^7_{\alpha\beta}(p_2) \ . \tag{4.26}$$

For the fermion diagrams the Ward identity is trivially satisfied in a QED-like fashion. For the rest of the vertex diagrams that have not been treated thus far, the result of their contraction with q^μ gives zero on shell. Adding all relevant equations together we arrive at the advertised Ward identity of Eq. (4.1), a major result of this paper. It is important to notice that the pinch contributions have been instrumental for the validity of Eq. (4.1).

V. MAGNETIC DIPOLE AND ELECTRIC QUADRUPOLE MOMENTS OF THE W

In the last two sections we constructed the gauge-independent γW^+W^- vertex and we proved the Ward identity it satisfies. In this section we will proceed to extract from this vertex its contributions to the magnetic dipole μ_W and electric quadrupole Q_W. Following the parametrization of Eqs. (1.4) and (1.5), we need to determine the quantities $\Delta\kappa_\gamma$ and ΔQ_γ, or equivalently κ_γ and λ_γ. Since they originate from the new γW^+W^- vertex they will be manifestly gauge independent. The restoration of the gauge independence of the final answer results in *automatically* two additional very important improvements; unlike the expressions for the bosonic contributions to $\Delta\kappa_\gamma$ recorded in [7], the respective quantities derived in this section are (a) infrared finite and (b) well behaved for high values of the momentum Q^2.

Specifically, regarding point (b), we show that $\hat{\Delta}\kappa_\gamma \to 0$ as $Q^2 \to \infty$; this is to be contrasted to the asymptotic behavior of the respective expression given in [7], which, due to the presence of gauge-dependent contributions, appeared to violate perturbative unitarity. It is important to emphasize that, as we explicitly demonstrate in this section, all the pathologies listed above, which appear to be artifacts inextricably connected to gauge dependences, are immediately cured once the S-matrix pinch technique is used, without *any* further assumptions.

As we explained in Sec. III, the new gauge-invariant vertex is built up from the usual vertex diagrams calculated in the Feynman–'t Hooft gauge and the vertexlike pinch contributions we extract from box diagrams. So, if we denote by $\Delta\kappa_\gamma^{(\xi=1)}$ and $\Delta Q_\gamma^{(\xi=1)}$, respectively, the contributions of the usual vertex diagrams ($\xi=1$), by $\Delta\kappa_\gamma^P$ and ΔQ_γ^P the analogous contributions of the pinch parts, and use carets ($\hat{\Delta}\kappa_\gamma$ and $\hat{\Delta}Q_\gamma$) to indicate the new *gauge-independent* quantities, we clearly have the relations

$$\hat{\Delta}\kappa_\gamma = \Delta\kappa_\gamma^{(\xi=1)} + \Delta\kappa_\gamma^P \tag{5.1}$$

and

$$\hat{\Delta}Q_\gamma = \Delta Q_\gamma^{(\xi=1)} + \Delta Q_\gamma^P \ . \tag{5.2}$$

The task of actually calculating $\hat{\Delta}\kappa_\gamma$ and $\hat{\Delta}Q_\gamma$ is greatly facilitated by the fact that the quantities $\Delta\kappa_\gamma^{(\xi=1)}$ and $\Delta Q_\gamma^{(\xi=1)}$ have already been calculated in [7]. It must be emphasized however that the expression for $\Delta\kappa_\gamma^{(\xi=1)}$ (but not $\Delta Q_\gamma^{(\xi=1)}$) is infrared *divergent* for $Q^2 \neq 0$ due to the presence of the following double integral over the Feynman parameters (t,a), given in Eq. (26), of [7]:

$$\begin{aligned} R &= -\left[\frac{\alpha_\gamma}{\pi}\right]\frac{Q^2}{M_W^2}\int_0^1 da \int_0^1 \frac{dtt}{t^2-t^2(1-a)a(4Q^2/M_W^2)} \\ &= -\left[\frac{\alpha}{2\pi}\right]\frac{Q^2}{M_W^2}\int_0^1 \frac{da}{1-(1-a)a\,(4Q^2/M_W^2)}\int_0^1 \frac{dx}{x} \ , \end{aligned} \tag{5.3}$$

which originates from the graph of Fig. 4 (1,2), when one of the internal propagators is a virtual photon. ($\alpha_\gamma \equiv e^2/4\pi$ is the fine structure constant.)

We only need therefore to determine the expressions for ΔQ_γ^P and $\Delta\kappa_\gamma^P$; this is equivalent to determining the pinch contributions to the functions $a_1(Q^2), a_2(Q^2)$, and $a_3(Q^2)$ defined in Eq. (1.6), which we will call $a_1^P(Q^2)$, $a_2^P(Q^2)$, and $a_3^P(Q^2)$. For on-shell W^+ and W^- pinch contribution originate only from the $B_{\mu\alpha\beta}^V$ term in Eq. (3.17). To establish contact with [7], we use the following identity to parametrize the denominator of the integrals:

$$\frac{1}{ABC} = \int_0^1 da \int_0^1 dt \frac{2t}{\{[A(1-a)+Ba]t+[C(1-t)]\}^3} \ . \tag{5.4}$$

The momentum integration can be immediately performed (We remind the reader that $B_{\mu\alpha\beta}$ is ultraviolet finite, so no regularization is needed.) In the limit of interest, namely $p_1^2 = p_2^2 = M_W^2$, we find

$$B_{\mu\alpha\beta}^V = -\frac{1}{2}\frac{\alpha_V}{4\pi}\frac{q^2}{M_W^2}\int_0^1 da \int_0^1 (2tdt)\frac{F_{\mu\alpha\beta}}{L_V^2} \ , \tag{5.5}$$

with $\alpha_V = g_V^2/4\pi$ and

$$\begin{aligned} F_{\mu\alpha\beta} &= (\tfrac{3}{2}+at)g_{\alpha\beta}(p_1-p_2)_\mu + (3at+2)g_{\beta\mu}p_{2_\alpha} \\ &\quad -(3at+2)g_{\beta\mu}p_{1_\beta} \\ &= 2(\tfrac{3}{2}+at)g_{\alpha\beta}\Delta_\mu + 2(3at+2)[g_{\alpha\mu}Q_\beta - g_{\beta\mu}Q_\alpha] \end{aligned} \tag{5.6}$$

and

$$\begin{aligned} L_V^2 &= t^2 - t^2 a(1-a)\left[\frac{q^2}{M_W^2}\right] + (1-t)\frac{M_V^2}{M_W^2} \\ &= t^2 - t^2 a(1-a)\left[\frac{4Q^2}{M_W^2}\right] + (1-t)\frac{M_V^2}{M_W^2} \end{aligned} \tag{5.7}$$

from which immediately follows that

$$a_1^P(Q^2) = -\frac{1}{2}\frac{Q^2}{M_W^2}\sum_V \frac{\alpha_V}{\pi}\int_0^1 da \int_0^1 (2tdt)\frac{2(3/2+at)}{L_V^2} \ , \tag{5.8}$$

$$a_2^P(Q^2) = -\frac{1}{2}\frac{Q^2}{M_W^2}\sum_V \frac{\alpha_V}{\pi}\int_0^1 da \int_0^1 (2tdt)\frac{2(2+3at)}{L_V^2} \tag{5.9}$$

and since there is no term proportional to $\Delta_\mu Q_\alpha Q_\beta$ in Eq. (5.6),

$$a_3^P(Q^2) = 0 \ . \tag{5.10}$$

So, using Eqs. (1.7) and (1.8) we have, for $\Delta\kappa_\gamma^P$ and ΔQ_γ^P,

$$\Delta\kappa_\gamma^P = -\frac{1}{2}\frac{Q^2}{M_W^2}\sum_V \frac{\alpha_V}{\pi}\int_0^1 da \int_0^1 (2tdt)\frac{(at-1)}{L_V^2} \tag{5.11}$$

and

$$\Delta Q_\gamma^P = 0 \ . \tag{5.12}$$

It is important to notice that even though $\Delta Q_\gamma^P = 0$ *both* μ_W and Q_W will assume values different than those predicted in the $\xi=1$ gauge. That this is so may be seen from Eqs. (1.3) and (1.2); clearly, even though the value of λ_γ does not change, the value of κ_γ changes, and this change affects both μ_W and Q_W through Eqs. (1.4) and (1.5). In the expression given in Eq. (5.11) the first term (for $V=Z$) is infrared finite (since $M_Z \neq 0$), whereas the second term (for $V=\gamma$) is infrared divergent, since $M_\gamma = 0$. Calling this second term Θ we have

$$\begin{aligned} \Theta &= -\frac{1}{2}\left[\frac{\alpha_\gamma}{\pi}\right]\frac{Q^2}{M_W^2} \\ &\quad \times \int_0^1 da \int_0^1 dt \frac{2t(at-1)}{t^2[1-a(1-a)(4Q^2/M_W^2)]} \ , \end{aligned} \tag{5.13}$$

which can be rewritten as

$$\Theta = -R - \left[\frac{\alpha_\gamma}{\pi}\right]\frac{Q^2}{M_W^2}\int_0^1 da \frac{a}{1-a(1-a)(4Q^2/M_W^2)} , \tag{5.14}$$

where R is the infrared divergent integral defined in Eq. (5.3). On the other hand, the second term in Eq. (5.14), is infrared finite. Clearly, including the first term of Eq. (5.14) in the value of $\hat{\Delta}\kappa_\gamma$ *exactly* cancels the infrared divergent contribution of Eq. (5.3), thus giving rise to an infrared finite expression for $\hat{\Delta}\kappa_\gamma$. So, after the infrared divergent part of Eq. (5.13) is canceled, $\Delta\kappa_\gamma^P$ is given by the expression

$$\Delta\kappa_\gamma^P = \Theta_\gamma + \Theta_Z \tag{5.15}$$

with Θ_γ the second term in Eq. (5.14), and Θ_Z the second term in Eq. (5.11), namely

$$\Theta_\gamma = -\left[\frac{\alpha_\gamma}{\pi}\right]\frac{Q^2}{M_W^2}\int_0^1 da \frac{a}{1-a(1-a)(4Q^2/M_W^2)} \tag{5.16}$$

and

$$\Theta_Z = -\frac{Q^2}{M_W^2}\left[\frac{\alpha_Z}{\pi}\right]\int_0^1 da \int_0^1 dt \frac{t(at-1)}{L_Z^2} \tag{5.17}$$

and, from Eq. (5.1),

$$\hat{\Delta}\kappa_\gamma = [\Delta\kappa_\gamma^{(\xi=1)}]_{if} + \Theta_\gamma + \Theta_Z , \tag{5.18}$$

where the subscript (if) in the first term of the RHS indicates that the contribution from the $\xi=1$ gauge is now genuinely infrared finite (the authors of [7] removed the infrared divergent contribution by hand). Finally, the magnetic dipole moment μ_W and electric quadrupole moment Q_W are given by

$$\mu_W = \frac{e}{2M_W}(2+\hat{\Delta}\kappa_\gamma) \tag{5.19}$$

and

$$Q_W = -\frac{e}{M_W^2}(1+\hat{\Delta}\kappa_\gamma+2\hat{\Delta}Q_\gamma) . \tag{5.20}$$

Both $\Delta Q_\gamma^{(\xi=1)}$ and $\Delta\kappa_\gamma^{(\xi=1)}$ have been computed numerically in [7]. We now proceed to compute the integrals in Eqs. (5.16) and (5.17), which determine $\Delta\kappa_\gamma^P$. It is elementary to evaluate Θ_γ. Setting $\Theta_\gamma = -(\alpha_\gamma/\pi)\hat{\Theta}_\gamma$ we have

$$\hat{\Theta}_\gamma = \begin{cases} \dfrac{2}{\Delta}\left[\arctan\left[\dfrac{1}{\Delta}\right] - \arctan\left[\dfrac{-1}{\Delta}\right]\right] & \text{for } Q^2 < M_W^2 , \\ -4 \text{ for } Q^2 = M_W^2 , \\ \dfrac{2}{\Delta}\ln\left[\dfrac{|\Delta-1|}{\Delta+1}\right] & \text{for } Q^2 > M_W^2 , \end{cases} \tag{5.21}$$

for spacelike Q^2, where $\Delta = \sqrt{|M_W^2/Q^2 - 1|}$, and

$$\hat{\Theta}_\gamma = \frac{2}{\Delta}\ln\left[\frac{|\Delta-1|}{\Delta+1}\right] \tag{5.22}$$

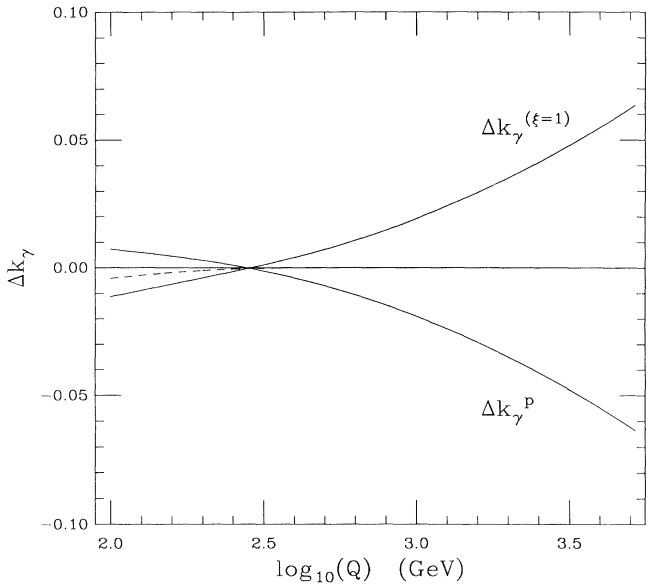

FIG. 10. The bosonic contribution $\hat{\Delta}\kappa_\gamma$ to the W magnetic dipole moment for timelike momenta. The dashed line corresponds to $\hat{\Delta}\kappa_\gamma$ and is the sum of the two solid lines. Notice that the dashed line approaches zero asymptotically.

for timelike Q^2, where $\Delta = \sqrt{(M_W^2/|Q^2|)+1}$.

The double integral Θ_Z can, in principle, be expressed in a closed form in terms of Spence functions (see for example [22]); instead, we find it more convenient to evaluate this integral numerically, after performing the first integration exactly. The momentum variable Q is defined as $Q \equiv \mathrm{sgn}(Q^2)\sqrt{|Q^2|}$. We used the same values for the

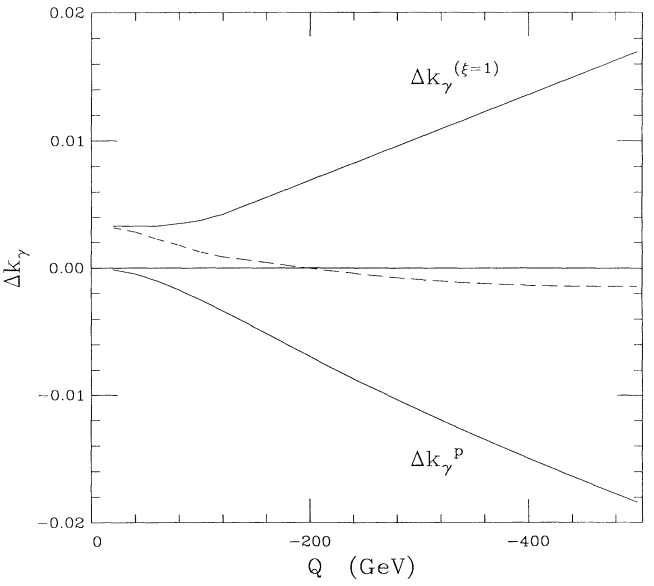

FIG. 11. The bosonic contribution $\hat{\Delta}\kappa\gamma$ to the W magnetic dipole moment for spacelike momenta. The final answer (dashed line) approaches zero asymptotically.

TABLE I. The values of $\hat{\Delta}\kappa_\gamma$ for timelike Q^2.

Q (GeV)	(10^{-4}) $\hat{\Delta}\kappa\gamma$
100	−42.0
120	−32.1
140	−24.5
160	−18.7
180	−14.3
200	−11.0
220	−8.5
240	−6.5
260	−5.0
280	−3.8
300	−3.0
320	−2.3
340	−1.8
360	−1.5
380	−1.2
400	−1.0
420	−0.9
440	−0.8
500	−0.7

TABLE II. The values of $\hat{\Delta}\kappa_\gamma$ for spacelike Q^2.

Q (GeV)	$(\times 10^{-4})$ $\hat{\Delta}\kappa\gamma$
−20	31.8
−40	28.2
−60	22.8
−80	17.8
−100	12.3
−120	8.6
−140	6.5
−160	4.2
−180	2.0
−200	0.2
−220	−2.3
−240	−4.2
−260	−5.9
−280	−7.6
−300	−9.0
−320	−10.2
−340	−11.3
−360	−12.2
−380	−12.9
−400	−13.5
−420	−13.9
−440	−14.2
−460	−14.4
−480	−14.3
−500	−14.2

constants appearing in our calculations as in [7], namely $\alpha_\gamma=\frac{1}{128}$, $M_W=80.6$ GeV, $M_Z=91.1$ GeV and $s^2=0.23$. As in [7], we only consider the real contributions of the integrals.

The result of the computation is rather interesting, at least from the theoretical point of view. $\Delta\kappa_\gamma^P$, which originates from pinching box diagrams, furnishes exactly the contributions needed to restore the unitarity of the final answer. Indeed, as the authors of [7] emphasized, $\Delta\kappa_\gamma^{(\xi=1)}$ is an increasing function of Q^2, which essentially reflects the fact that $\Delta\kappa_\gamma^{(\xi=1)}$ is by itself *not* a gauge invariant object in the limit $Q^2\to\infty$, where the local SU(2)×U(1) is restored. As we show in Fig. 10, for large values of Q^2, $\Delta\kappa_\gamma^P$, is nearly equal in magnitude and opposite in sign to $\Delta\kappa_\gamma^{(\xi=1)}$. Therefore, when according to Eq. (5.1) both contributions are added, the resulting expression for $\hat{\Delta}\kappa_\gamma$ approaches zero asymptotically, as $Q^2\to\infty$. The same mechanism of unitarity restoration takes place for $Q^2\to-\infty$. (See Fig. 11).

For completeness, we record in Tables I and II, several values of the final answer for $\hat{\Delta}\kappa_\gamma$, for timelike and spacelike values of Q^2, respectively. Its numerical contribution is comparable to the respective contributions from fermion and Higgs graphs; its relevance will clearly depend on the accuracy achieved in the next generations of experiments. Regardless of that, however, from the theoretical point of view our results augment those of [7], rendering them gauge fixing parameter independent, infrared finite, and asymptotically well-behaved, in a natural way.

VI. CONCLUSIONS

In this paper we have undertaken a study of the structure of the trilinear gauge boson vertices in the context of the standard model. Using the S-matrix pinch technique we constructed to one-loop order gauge-independent γWW and ZWW vertices, with all three incoming momenta off shell. In the limit $p_1^2, p_1^2\to M_W^2$ the gauge-independent vertices give rise to expressions for the magnetic dipole moment μ_W and electric quadrupole moment Q_W, which, unlike previous treatments, are suitable for comparison with experimental observation [23]. The main effect of the pinch contributions is to render the results gauge independent, infrared finite, and asymptotically well-behaved, while their numerical contribution to the final answer turned out to be small.

The gauge-independent off-shell γW^+W^- vertex was shown to satisfy a simple QED-like Ward identity, which relates it to the gauge-independent W self-energies introduced by Degrassi and Sirlin. It would be interesting to determine whether or not the gauge-independent ZW^+W^- vertex satisfies a similar Ward identity. Calculations in this direction are already in progress.

ACKNOWLEDGMENTS

The authors are indebted to Professor A. Sirlin for many useful discussions, and to A. Bunch and T. Battacharya for technical support. This work was supported in part by the National Science Foundation under Grant No. PHY-9017585.

[1] A. Sirlin, talk at the SUSY 93 International Workshop, Boston, Massachusetts (unpublished).
[2] K. J. F. Gaemers and G. J. Gounaris, Z. Phys. C **1**, 259 (1979).
[3] K. Hagiwara *et al.*, Nucl. Phys. **B282**, 253 (1987).
[4] U. Baur and D. Zeppenfeld, Nucl. Phys. **B308**, 127 (1988).
[5] U. Baur and D. Zeppenfeld, Nucl. Phys. **B325**, 253 (1989).
[6] E. N. Argyres *et al.*, Phys. Lett. B **272**, 431 (1991).
[7] E. N. Argyres *et al.*, Nucl. Phys. **B391**, 23 (1993).
[8] W. A. Bardeen, R. Gastmans, and B. Lautrup, Nucl. Phys. **B46**, 319 (1972).
[9] J. M. Cornwall, in *Deeper Pathways in High Energy Physics,* edited by B. Kursunoglu, A. Perlmutter, and L. Scott (Plenum, New York, 1977), p. 583.
[10] J. M. Cornwall, Phys. Rev. D **26**, 1453 (1982).
[11] J. M. Cornwall, W. S. Hou, and J. E. King, Phys. Lett. **153B**, 173 (1988).
[12] S. Nadkarni, Phys. Rev. Lett. **61**, 396 (1988).
[13] J. M. Cornwall and J. Papavassiliou, Phys. Rev. D **40**, 3474 (1989).
[14] M. Lavelle, Phys. Rev. D **44**, 26 (1991).
[15] J. Papavassiliou, Phys. Rev. D **41**, 4728 (1993).
[16] J. Papavassiliou, Phys. Rev. D **41**, 3179 (1990).
[17] G. Degrassi and A. Sirlin, Phys. Rev. D **46**, 3104 (1992).
[18] In this paper we do not touch upon issues related to the gauge invariance of effective trilinear couplings stemming from theories beyond the standard model.
[19] This conserved form is, in fact, automatic in other forms of the pinch technique, e.g., the off-shell approach of Refs. [9] and [10], or the intrinsic pinch discussed in Ref. [13].
[20] A. Sirlin, Rev. Mod. Phys. **50**, 573 (1978).
[21] As explained in [16], in general additional contributions to the gauge-independent quantities under construction arise, when the S-matrix PT is applied for external fermions with different masses, such as massive electrons and massless neutrinos. It is easy to see, however, that, in the case at hand, all such contributions do *not* kinematically contribute to the definition of the three-vector-boson vertices, and they will be discarded anyway.
[22] G. 't Hooft and M. Veltman, Nucl. Phys. **B153**, 365 (1979).
[23] The general strategy of how to extract the experimental values of quantities such as $\Delta\kappa$ from the total scattering cross section has been outlined in G. Degrassi, A. Sirlin, and W. Marciano, Phys. Rev. D **39**, 287 (1989).